RSC Advances

ROYAL SOCIETY OF CHEMISTRY

www.rsc.org/advances

Switching selectivity between Pb^{2+} and Hg^{+2} ions through variation of substituents at xanthene end; 'turn-on' signalling responses by FRET modulation

Biswonath Biswal and Bamaprasad Bag*

Colloids and Materials Chemistry Department, Academy of Scientific and Innovative Research, CSIR-Institute of Minerals and Materials Technology, P.O.: R.R.L., Bhubaneswar-751 013, Odisha, India. Fax: (+) 91 674 258 1637; Tel: (+ 91) 674 237 9254, Email: *bpbag@immt.res.in*

Abstract

Few rhodamine based probes($\mathbf{L_1}$-$\mathbf{L_4}$) which consist of a similar 2-(aminoethyl)-pyridine unit at their carboxamide end but vary with substituents attached to N-atom at their xanthene end were synthesized. The rhodamine G based probes $\mathbf{L_1}$-$\mathbf{L_3}$ have shown preferential chromogenic and fluorogenic 'turn-on' spectral responses in presence of Pb^{2+} ion, where one of the two ethyl substituted secondary amino groups attached to xanthene core is either remained un-substituted (as in $\mathbf{L_1}$) or functionalized with a bulky aromatic group (as in $\mathbf{L_2}$) or an long alkyl chain (as in $\mathbf{L_3}$). On contrary, the probe $\mathbf{L_4}$ which incorporates two ethyl-substituents at both N-atoms attached to xanthene core has exhibited dual mode spectral amplification selectively in presence of Hg^{2+} ion. The reversible dual mode signalling pattern of bifluorophoric $\mathbf{L_2}$ selectively in presence of Pb^{2+} ion owe to perturbation of a combined PET(photo-induced electron transfer) inhibition and FRET (fluorescence resonance energy transfer) initiation processes. The observed ratiomeric signalling pattern enabled it to detect Pb^{2+} ions at low concentration level, even in living organisms such as *E. Coli*. The altered selectivity in signalling pattern infers to a modulated stereo-electronic environment for metal ion coordination, which in turn, owe to induced amine rigidity at xanthene end.

Introduction

The development of molecular probes for selective detection of various analyte of environmental and biological importance have attracted much attention[1] in past couple of decades relying highly on methodological approaches involving various binding sites, signalling subunits and operational principles, which concurrently able to display selective changes in photo-physical signatures upon guest binding. Transition and heavy metal ions being such targeted analytes, their on-site, real time, selective detection and analyses are highly desirable. Their presence or absence deviating requisite concentration threshold imparts lethal toxic effect[2] to cause serious human health hazards and environmental impacts although their existence in active sites of enzymes and proteins of living organism is highly essential to operate several biological functions. The toxic lead and mercury ion contaminations in environment which occur through various natural and human activities are a matter of concern. Intake of ionic lead even in ultra-trace quantity causes severe health problems[3] such as memory loss, anaemia, and slow nerve conduction velocity in children[4]. Exposure to mercury consequently leads to cell dysfunction[5] resulting in many physiological disorder[6] and other health hazards[7] because of its higher affinity for protein/enzymes based thiol- groups. Hence, selective detection of these two ions at very low concentration level has been indispensable for their impact assessment. Among many feasible and viable solutions, development of efficient chemosensory probes is promising owing to synthetic and operational advantages. Fluorescent probes are advantageous due to its highly selective, sensitive, quick response time and non-destructive nature. At the same time, chromogenic probes facilitate a visual perception of signalling behaviour as a mode of colour change. Thus, covalent architectures which undergo both fluorogenic and chromogenic signal modulation are preferable in designing molecular chemosensory probes. In this context, excellent spectroscopic features of xanthene based dyes along with contrast structure-function

correlation prompt it to be a prejudice choice[8] of signalling entity. Several rhodamine-based probes for selective detection of Hg^{2+} and Pb^{2+} ions have already been known[9,10] following their metal-induced spiro-cyclic ring-opening. With our quest on metal ion selectivity and signalling pattern of derivatized rhodamine chemosensors, we have recently demonstrated[11] few "amino-alkyl-amino" substituted rhodamine-B based probes to exhibit dual mode signalling selectively with Hg^{2+} ion among various metal ions in an organic-aqueous binary solvent. Such probes quite often lack in efficiency concerning sensitivity level of detection despite of advantages in dual mode signalling pattern, as a low signal to noise ratio in spectral amplification at very low concentration level of analyte restricts limit of detection. On contrary, a bi-fluorophoric ratiomeric probe incorporating rhodamine as one of the fluorophores should be promising in addressing sensitivity issues. It not only allow measurement of fluorescence intensities at two different wavelengths[12] along with increased dynamic[13] range, but also render a built-in correction for environmental effects in respect of smaller concentration variation. Since sensitivity and dynamic range of such probes are controlled by ratio of emission intensities, which lowers dependency of signal to noise ratio to achieve a higher sensitivity, the probe-metal ion interaction is crucial in exhibiting high ratiomeric signals. For a higher signalling efficiency, such interactions need to overcome various interactive yet detrimental parameters such as probe-solvent/metal ion-solvent interactions and hydration of metal ions etc. in order to induce selectivity in coordination. Thus, efficiency of probe-metal interaction can effectively be tuned through manipulation of stereo-electronic environment of spatially disposed donor atoms of receptor in a probe. Anticipating variation in electron density over donor atoms to result in altered coordination preferences of receptor, it is imperative to understand the effect of various substituents attached to rhodamine based probes on its coordination preferences towards metal ions, in turn, ability to open up its spiro- ring for dual mode signalling responses. Earlier reported[11,14]

substituted 'amino-alkyl-amino' coupled rhodamine B based probes although preferentially exhibited signalling responses[11] selectively with Hg^{2+} ion in organic aqueous medium irrespective of substitution at receptor unit, those were hardly observed to alter selectivity towards metal ion which coordinates to 'amino-alkyl-amide' segment at dye's spiro-lactam end. On the other hand, either none or only one alkyl group substitution at each N-donor atoms of xanthene unit as in rhodamine-G dye or even their rigidization with bulky group attachment lowers the activation of internal conversion process significantly[15]. Hence, in order to investigate stereo-electronic effect of further alkyl-/bulky aromatic substitution to mono ethyl- substituted amino groups (as in rhodamine G) on preferential metal ion coordination that initiates ring-opening process few such probes (**L_1-L_4**) were synthesized (Scheme 1) and their photophysical behaviour were investigated in presence of various metal ions. These probes consist of a 2-(aminoethyl) pyridine unit attached to their carboxamide end while incorporate varied alkyl- substitution to one of amino groups at xanthene end. With structural modifications, **L_1-L_3** probes contain rhodamine G core while **L_4** consist of rhodamine B moiety to execute signalling action. Further, the bifluorophoric signalling probe **L_2** consist of both anthracene and rhodamine G fluorophores in its architecture in 'Donor(Anthracene)-spacer(methylene)-Acceptor(rhodamine 6G) format in order to exhibit signalling action in a ratiomeric pattern through modulation of various simultaneously operative processes, predominantly metal ion induced photo-induced electron transfer (PET)[16,17] inhibition and subsequent initiation of intra-molecular fluorescence resonance energy transfer (FRET)[18-20] process. Rhodamine structures in spiro-cyclic conformation have an interrupted π-conjugation restricted within substituted-aniline of xanthene core, hence does not act as an energy acceptor. Its metal ion induced ring-opened form facilitates it to be a good energy acceptor, thus capable of triggering a FRET process. In an earlier report[20] on metal ion induced dual mode signalling of bifluorophoric probes incorporating rhodamine B

and anthracene couple as fluorophores attached to respective amino ends of bis-(amino-ethyl-piperazine) spacer, a weak FRET was observed to be operative due to poor spectral overlap between both fluorophores. In order to induce a higher order of energy transfer efficiency in such bifluorophoric donor-acceptor ensemble, factors such as their distance and orientation are essentially crucial besides a stronger spectral overlap. The choice of anthracene-rhodamine G couple in $\mathbf{L_2}$ is obvious as excited state emission spectra of donor(anthracene) largely overlaps with ground state absorption spectra of acceptor(rhodamine 6G), better than that with rhodamine B. In general, earlier design of rhodamine based probes with FRET operational principles for metal ion induced signal perturbation mostly incorporated both fluorophores discretely attached to both ends of the receptor unit, where rhodamine was coupled to the receptor at its spiro-cyclic end. Herein a different strategy of FRET based probe design has been followed as fabricated in $\mathbf{L_2}$, both fluorophores were coupled at amino groups attached to xanthene core with an anticipated FRET perturbation upon metal ion coordination to receptor unit at lactonized end. With all these methodological prejudices, photophysical investigations of $\mathbf{L_1}$-$\mathbf{L_4}$ in presence of metal ions have been envisaged to exhibit altered preferences in their dual mode signalling pattern as a function of varied stereo-electronic situation. The 2-(aminoethyl)-pyridine derivatized rhodamine G based probe $\mathbf{L_1}$ herein reported to exhibit selectivity towards Pb^{2+} ion which remained unaltered on its derivatization at one of its amino group attached to xanthene unit with either an octyl-substitution (as in $\mathbf{L_3}$) or methyl-anthracene substitution(as in $\mathbf{L_2}$) to operate through a combined PET-FRET process modulation. However, probe $\mathbf{L_4}$ which is a rhodamine-B analogue of $\mathbf{L_1}$ exhibited dual mode signalling selectively with Hg^{2+} ion substantiating the effect of structural modification on tuning their preferences towards metal ion coordination. These chemosensors are also expected to have high sensitivity, selectivity, reversibility and

operation under physiological pH for possible applications such as fluorescence imaging of metal ions in living cells for their in-situ detection at a low concentration level.

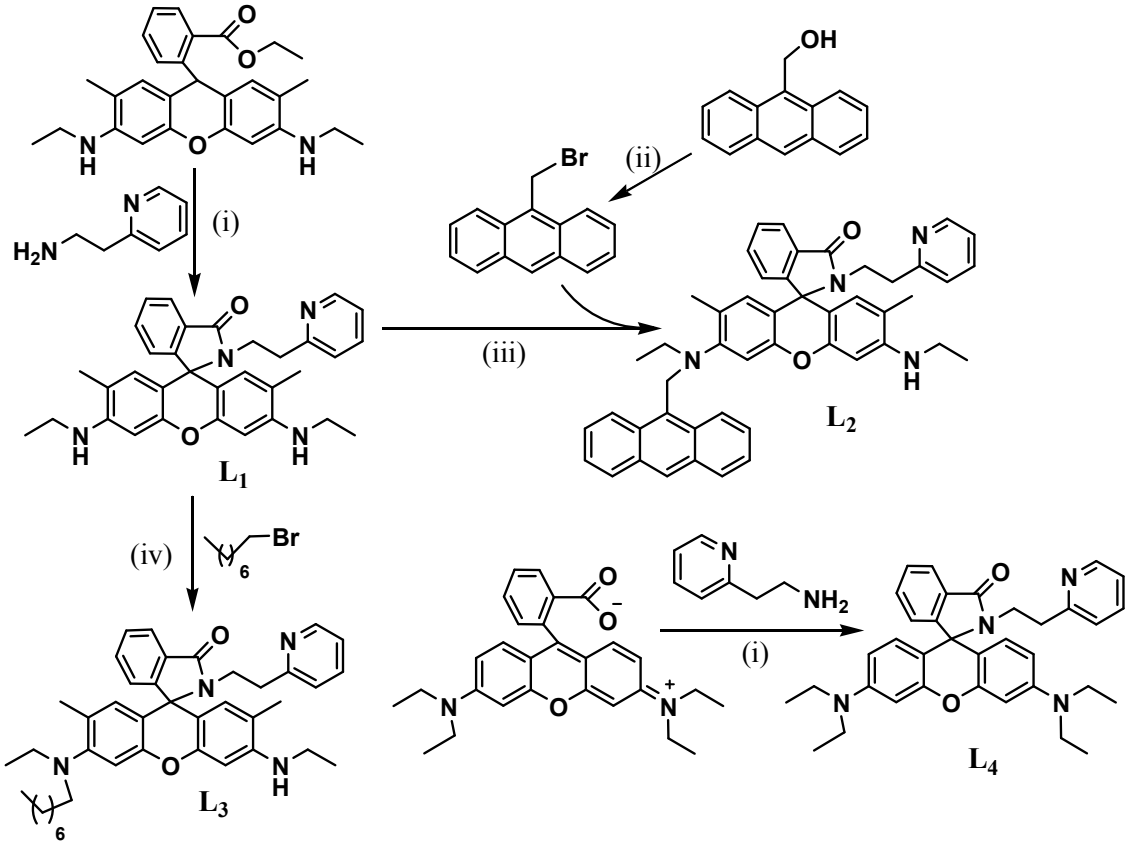

Reaction Conditions: (i) 2- aminoethyl pyridine, EtOH, reflux, 6h.; (ii) PPh_3, Br_2, MeCN, RT, 1h.; (iii) 9-Bromomethyl anthracene, toluene, Et_3N, reflux, 4h.; (iv) 1-bromo-octane, toluene, Et_3N, reflux, 8h.

Scheme 1: Synthetic route to probes $\mathbf{L_1}$, $\mathbf{L_2}$, $\mathbf{L_3}$ and $\mathbf{L_4}$.

Results and discussion

The probes($\mathbf{L_1}$-$\mathbf{L_4}$) were synthesized as per the synthetic route depicted in Scheme 1. $\mathbf{L_1}$ was synthesized through condensation of Rhodamine 6G with 2-aminoethylpyridine. Its subsequent nucleophilic substitution(SN_2) reaction with 9-bromomethyl anthracene yielded $\mathbf{L_2}$ while resulted in $\mathbf{L_3}$ with 1-bromo-octane. Condensation of 2-aminoethylpyridine with rhodamine B yielded in $\mathbf{L_4}$ which further crystallized in ethanol to afford single crystals

suitable for X-ray diffraction through slow evaporation technique. All these probes were characterized by MS, ^{1}H NMR and ^{13}C NMR spectral analyses. The characteristic quaternary carbon peak near ~65 ppm in their ^{13}C-NMR spectrum in $CDCl_3$ ascertained predominant existence of rhodamine's spirolactam conformation. Similar to other derivatives, solutions of **L_1** - **L_4** in various organic solvents were also appeared colourless along with a weak fluorescence inferring to existence of spirolactam conformation. The single crystal X-ray diffracted structural analysis[‡] for **L_4** has also confirmed rhodamine's spiro-cyclic conformation (Fig. 1). The non-bonded N3----N4 distance and torsion angle(O2---N3---C31—N4) which constitute the coordination cavity for metal ion complexation was found to be 4.436 Å and 118.5° respectively in **L_4**.

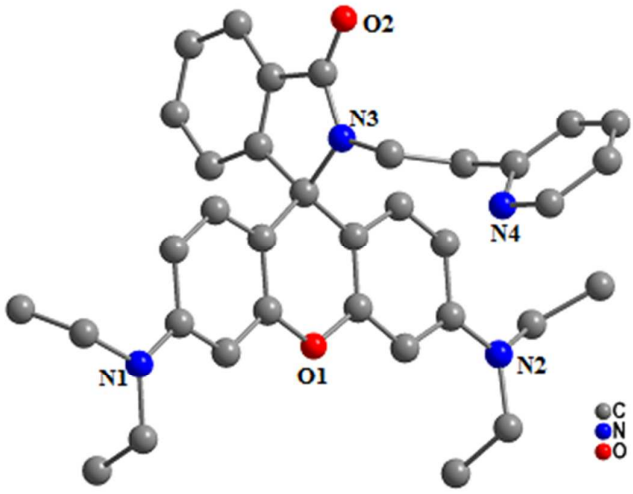

Fig. 1: Perspective view of the X-ray crystallographic structure of **L_4**. (H-atoms are omitted for clarity).

The UV-Vis absorption spectral pattern of **L_1-L_4** in various solvents revealed that these probes do not absorb in 500-600nm region due to spirolactam conformation of rhodamine and exhibited high energy ligand localized absorption transitions in 250-340nm region. Apart from this, the bifluorophoric probe **L_2** incorporating both rhodamine and anthracene fluorophores exhibited a characteristic peak of 9-alkyl substituted anthracene (0,0) absorption

transitions at 388nm along with its Frank-Condon vibrational structures at 368, 350, 333nm. Absence of any long range broad and structured band in its absorption spectra inferred that the lone pair electrons of donor N-atom did not interact with anthracene in their ground state, which was commonly observed[17] in many 'anthracene-methyl-amino' based probes.

Further, colourless solutions of **L_1-L_4** in acetonitrile-aqueous binary mixture exhibited either none or a weak fluorescence upon excitation of rhodamine dye (at 350/550nm) due to its spirolactam confirmation which facilitate[21] an intersystem crossing in its emissive CT state. The fluorescence of **L_2** was observed to be quenched due to various operative processes such as (a)PET from xanthene core to excited anthracene, (b)through bond ET from donor amino group to xanthene unit, (c)activated non-radiative pathways due to spiro-cyclic conformation of rhodamine, etc. The commonly observed[16,17] PET from *tert.*-amino donor to excited anthracene via methyl spacer might not be individually contributing much here because electron density over donor N-atom has drifted towards xanthene core inducing a partial double bond character to preferably prevail a through bond electron transfer, although contributions of such operative processes may not be completely overruled. It is worth mentioning here that partial derivatization of xanthene end amino groups of **L_1** with alkyl-substitution and induction of amine rigidity has envisaged activating internal conversion process. As a consequence, lowering in fluorescence for **L_2** and **L_3** was observed in comparison to that of **L_1**. Apart from non-radiative deactivation through internal conversion, operative photo-physical processes correlating to rhodamine's predominant spirolactam state have compelled these probes to exhibit an overall quenched fluorescence(ϕ_{FT}<0.001). It was further observed from spectral responses of **L_1-L_4** in EtOH at different temperatures (30 °C and 70 °C) that their spiro-cyclic conformation has been retained at lower temperatures (at<30 °C). At an elevated temperature (70 °C), probes such as **L_1** and **L_3** exhibited spectral enhancement due to ring-opening where as **L_2** and **L_4** remained in spirocyclic state inducing

none or negligible spectral changes. This indicate that an through bond electron transfer is favoured at an elevated temperatures in probes(**L_1-L_3**) where one of the amino groups attached to xanthene core is derivatized, which consequently enhance CT character though induced conjugation. However, deviation of spectral behaviour of **L_2** from its other analogues (**L_1** and **L_3**) at elevated temperatures is more complicated and needs further investigation on various operative processes before rendering any conclusion in this regard.

In order to investigate their metal ion induced signalling responses, various transition and heavy metal ions were added to the solution of **L_1-L_4** in aqueous-acetonitrile binary mixture. The choice of solvent is prejudiced here as presence of aqueous component in a medium has already been known to render functional selectivity in metal ion induced dual mode signalling in rhodamine-B based probes[11] correlating through competitive parameters such as probe-metal ion interaction and hydration energy of metal ions. Addition of various metals ions to the colourless solution of **L_1** in CH_3CN-H_2O (9.5: 0.5 v/v) has resulted in appearance of an absorption peak at 527nm with subsequent change in colour to orange in presence of Pb^{2+} (ε = 40768 dm^3 $mol^{-1}cm^{-1}$, $\varepsilon/\varepsilon_0$=59.2 fold), although few other metal ions also have induced appreciable changes (Ni^{2+}, $\varepsilon/\varepsilon_0$=18.6 fold) despite to a lesser extent in comparison to that due to Pb^{2+} ion. Its metal ion induced change in fluorescence (I_{555}) spectral pattern followed its absorption spectral behaviour, exhibited optimal fluorescence enhancement (ϕ_{FT} = 0.632) in presence of Pb^{2+} ion. These spectral amplifications along with subsequent appearance of colour in **L_1** is attributed to complexation-induced transformation of rhodamine's spiro-ring to its ring-opened carboxamide conformation, and extent of dual mode signalling was observed to be maximum in preferential presence of Pb^{2+} ion over other metal ions under investigation.

The absorption and emission spectral pattern of **L_2** (1μM) in CH_3CN-H_2O (9.5: 0.5 v/v) is shown in Fig. 2. None of these metal ions were observed to either induce any change in

colour of the solution or modulate of absorption transitions except Pb^{2+}, which on addition turned the colourless solution into orange along with appearance of an absorption transition at ~530nm corresponding to ring-opened rhodamine(Fig. 2a). When excited at 350nm, its quenched fluorescence (ϕ_{Rho}<0.001) also simultaneously enhanced ($\phi_{Rho(\mathbf{L2+Pb(II)})}$= 0.583) with fluorescence transition at ~555nm upon addition of Pb^{2+} (10eq.). The Pb^{2+}-induced fluorescence enhancement is attributed to perturbation of various interactive processes occurring simultaneously such as its coordination at carboxamide-pyridine receptor cavity enabling the spiro-lactam to open, consequent suppression of operative PET favouring a charge transfer conjugated channel involving xanthene core and subsequent initiation of a FRET from excited anthracene to ring-opened rhodamine. When monitored at anthracene emission window (I_{417}), Pb^{2+} ion did not induce substantial spectral enhancement in comparison to that for rhodamine moiety; its fluorescence from excited anthracene component hardly resulted in 2-fold enhancement in presence of Pb^{2+} ion through an anticipated PET suppression and still remained lower due to initiated FRET pathways. In context of anthracene monomer fluorescence, maximum enhancement was observed in presence of Cu^{2+} ion(ϕ_{An}= 0.159) among all metal ions added. The Pb^{2+} selective fluorescence enhancement in $\mathbf{L_2}$ as a consequence of combined PET inhibition-FRET initiation processes could not be observed for other metal ions, complementing inferences that from its absorption spectral analysis.

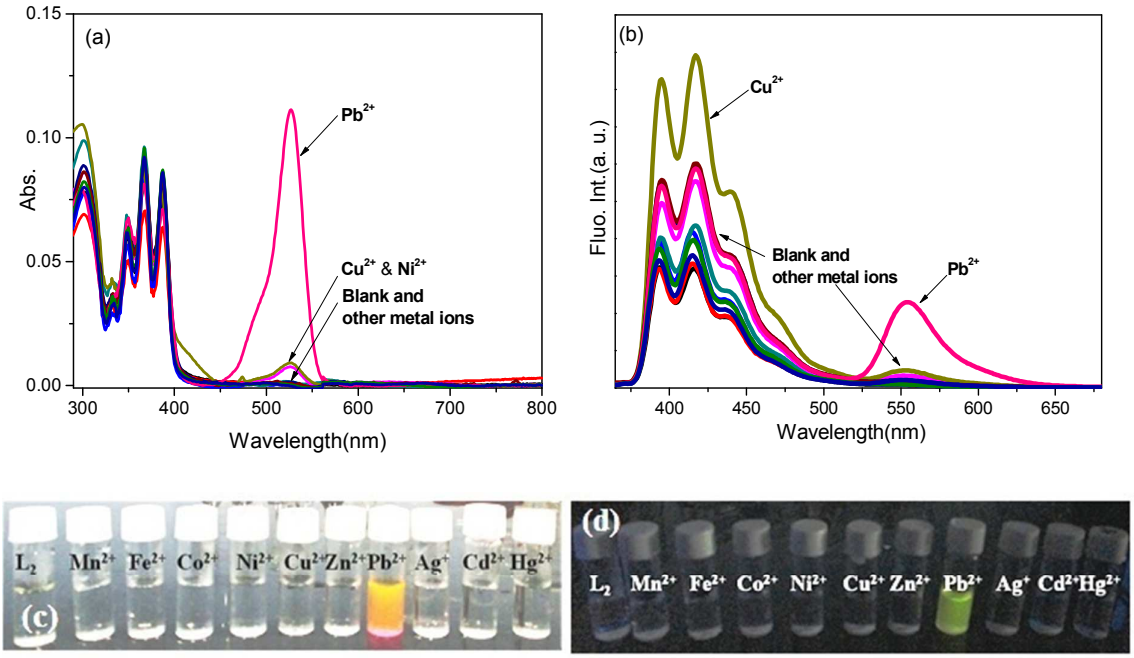

Fig. 2. Absorption (a) and fluorescence (b) spectra of $\mathbf{L_2}$ in presence of various metal ions in CH_3CN-H_2O (9.5:0.5 v/v), corresponding photographs showing colour change(c) and fluorescence on excitation at 350nm(d). [$\mathbf{L_2}$] = 1μM.

The fluorescence titration of $\mathbf{L_2}$ (0.1 μM) with Pb^{2+} in MeCN-H_2O (9.5: 0.5 v/v) revealed that it exhibited metal ion induced fluorescence enhancement in a ratiometric pattern with an isobestic point at ~515nm (Fig. 3). The fluorescence spectra of metal free $\mathbf{L_2}$ represented a structured band centred at 350-500nm region corresponding to weak fluorescence (ϕ_{An} = 0.0002) of excited anthracene and did not contain any long range transition corresponding to lactonized rhodamine G component. Upon gradual addition of Pb^{2+} ion to that solution, fluorescence intensity (I_{417}) corresponding to anthracene have enhanced (up to 2-fold) indicating inhibition in PET process; the increasing trend was observed up to addition of 20ppb concentration. Further addition up to 40ppb of Pb^{2+} resulted in decrease in anthracene fluorescence, however, gradual appearance of a new red-shifted emission peak at 555nm (Fig. 3a) corresponding to that of ring-opened rhodamine was observed with concomitant colour change from colourless to orange/green(under illumination at 350 nm). The decrease in I_{417} and increase in I_{555} fluorescence was observed in a ratiomeric fashion in 20-100 ppb

concentration range of added Pb^{2+} (Fig. 3b), which logistically supplemented initiation of FRET process.

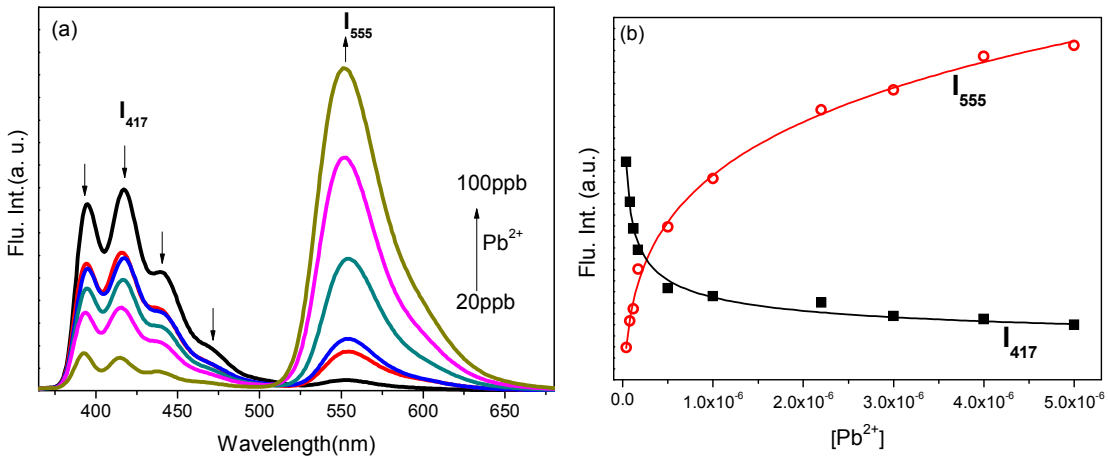

Fig. 3 (a) Fluorescence titration spectra of $\mathbf{L_2}$ (0.1 μM) upon gradual addition of Pb^{2+} ions in CH_3CN-H_2O (9.5:0.5 v/v), λ_{ex}= 350nm, em. and ex. b. p. = 5nm, RT; (b) Plot of its fluorescence intensities at 417nm and 555nm as a function of added Pb^{2+} ion concentration.

The plot of absorbance of $\mathbf{L_2}$ as a function of mole fractions of added Pb^{2+} ion (Job's plot) inferred the complexation stoichiometry to be in 1:1($\mathbf{L_2}$: Pb^{2+}) ratio. The nonlinear regression of its fluorescence titration data with Pb^{2+} ions has determined[22] association constant [log K_a =6.22 ± 0.24] of the complex. When estimated from its absorption titration spectral data, it was found (K_a^{abs} = 2.312 × 10^4 M^{-1}) to be consistent with that obtained through fluorescence titration profile and are comparable with a correlation factor [log {k_a(fluorescence)/k_a(absorption)}] of 1.42.

The appreciable spectral overlap between emission of excited anthracene and absorption of $\mathbf{L_2}$-Pb^{2+} complex with ring-opened rhodamine 6G conformation enabled these two fluorophores to be a donor(D_{An})-acceptor(A_{Rh}) pair for a FRET process. The efficiency of singlet-singlet excitation energy transfer (η_{EET}) between D_{An} to A_{Rh} evaluated[23] from its steady-state fluorescence data was found to be 90.35% and is in good agreement with other

rhodamine based systems[24]. The energy transfer efficiency depends upon Förster critical radius[25] (R_0) and on the interchromophoric distances (r) between D_{An} and A_{Rh}, where the energy transfer is effective over a distance of $R_0 \pm 0.5R_0$. Forster's critical distance (R_0) was calculated to be 41.16 Å by assuming rapid relative orientation of D_{An} and A_{Rh} with dynamic isotropic average of the orientation factor $<\kappa^2>$ as 2/3.

The quenched fluorescence of metal free $\mathbf{L_1}$, as mentioned, was observed to get decreased further upon partial substitution to one of amino groups attached to its xanthene core with an octyl chain (as in $\mathbf{L_3}$). This inferred that amino rigidity through partial derivatization induces activation of internal conversion process in these probes leading to further quenching of fluorescence. Among in presence of various metal ions under investigation in CH_3CN-H_2O(9.5:0.5 v/v) mixed medium, Pb^{2+} selectively rendered appearance of an absorption transition at ~525nm(ε = 120171 dm^3 mol^{-1} cm^{-1}) along with enhancement fluorescence at ~550nm (λ_{ex} = 525nm) in $\mathbf{L_3}$ while other metal ions rendered no or negligible change. Its colourless solution also turned orange which appeared green on illumination (at 350nm) selectively in presence of Pb^{2+} ion. The fluorescence enhancement in presence of Pb^{2+} was observed to be higher in $\mathbf{L_1}$(325 fold) in comparison to that in $\mathbf{L_2}$(28 fold) and $\mathbf{L_3}$ (24 fold).

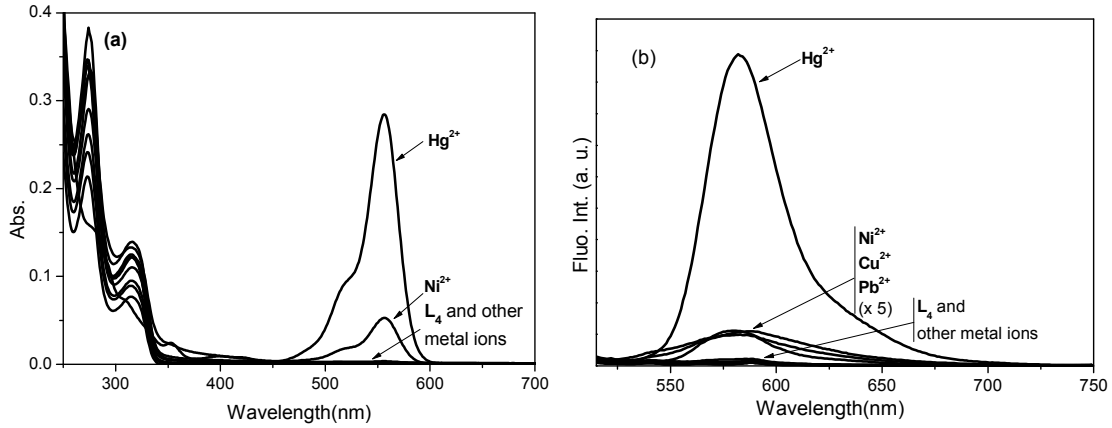

Fig. 4: (a) Absorption and (b)fluorescence spectra of $\mathbf{L_4}$ in absence and presence of various metal ions in CH_3CN-H_2O (9.5:0.5v/v), λ_{ex}= 500nm, em. and ex. bp = 5nm, RT, [$\mathbf{L_4}$] = 10μM (abs), 1μM (fluo), [M^{2+}] = 50 μM.

The Probe **L_4**, a rhodamine B analogue of **L_1**, was anticipated to show a longer wavelength absorption and emission in comparison to the later. Its fluorescence was also observed to be lowered(ϕ_F<0.001) owing to activated internal conversion process due to ethyl substitutions to both amino groups attached to xanthene core of **L_1**. On contrary to the metal ion induced spectral modulation in **L_1**, its photo-physical properties in absence and presence of various metal ions in MeCN-H_2O (9.5: 0.5 v/v) medium revealed that selective addition of Hg^{2+} ion resulted in absorption(ε_{555}=28125 $dm^3mol^{-1}cm^{-1}$) and fluorescence(ϕ_F = 0.591) 'turn-on' signalling responses, while presence of other metal ions did not induce any appreciable change on its absorption and fluorescence intensity (Fig. 4). The Hg^{2+} ion selective dual mode spectral amplification in **L_4** is consistent with those observed for other rhodamine B based probes in aqueous-acetonitrile mixture solvent and attributed to a prevailing Hg^{2+}–**L_4** interaction over hydration of Hg^{2+}. Other metal ions failed to exhibit such changes as their hydration was favoured over probe-metal ion interaction under the investigating conditions. The plot of absorbance against mole fractions of Hg^{2+} added to **L_4** inferred a 1:1 complexation stoichiometry and the association constant of complexation was estimated to be 2.6×10^4 M^{-1} from its absorption titration spectra and is comparable with that of **L_2**-Pb^{2+} complex (Fig. 5). However, the fluorescence titration profile of **L_4** with Hg^{2+} in MeCN-H_2O (9.5: 0.5 v/v) resulted in a higher association constant for the complex (log K_a^{flu} = 11.64) and is correlated with that obtained from absorption titration through a factor [log {k_a(fluo)/k_a(abs)}] of 2.63.

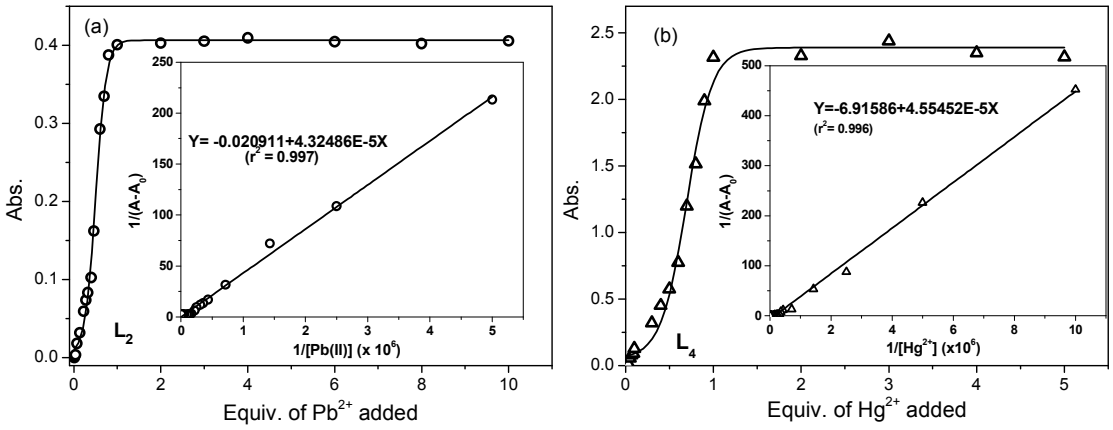

Fig. 5: Plot of absorption transition of (a) $\mathbf{L_2}$ (A_{527}) and (b) $\mathbf{L_4}$ (A_{555}) as a function of equivalents of added metal ions in CH_3CN-H_2O(9.5:0.5v/v). [$\mathbf{L_2}$] = 1×10^{-5}M, [$\mathbf{L_4}$] = 1×10^{-4}M. (Inset a & b): double reciprocal plot of absorption{$1/(A-A_0)$} against concentration of respective metal ions.

In order to comprehend impact of solvents on preferences of these rhodamine G based probes towards metal ion coordination that induces dual mode signalling, photo-physical behaviour of $\mathbf{L_2}$ (10μM) was also investigated in presence of various metal ions in pure CH_3CN. Its absorption and emission spectral pattern revealed that the probe does not have any preferences towards metal ions in their coordination induced signalling module in pure MeCN. Upon excitation at 350nm, it resulted in appearance of absorption spectral transition at 525nm due to spiro-ring opening of rhodamine-G moiety, simultaneously rendered colourless→ orange/green colour transition and triggered a FRET to exhibit fluorescence at 550nm in presence of few metal ions such as Fe^{2+} (ϕ_F = 0.91), Ni^{2+}(ϕ_F = 0.83), and Pb^{2+} (ϕ_F = 0.82) while other metal ions induced none or negligible spectral changes. A comparison in metal ion induced spectral modulation of $\mathbf{L_2}$ in pure CH_3CN with that in aqueous CH_3CN inferred that aqueous component in the solvent promoted its preferential coordination to Pb^{2+} ion over the metal ion's hydration. On contrary, presence of aqueous component in medium endorsed a preferential coordination of $\mathbf{L_4}$ to Hg^{2+} ion. These observations inferred that aqueous component in solvent composition plays a vital role in inducing functional

selectivity of metal ion in coordination mediated dual mode signalling, owing to competitive parameters such as metal–probe interaction against hydration of metal ions. Further, from fluorescence titration data of **L_2** with Fe^{2+} in dry CH_3CN, the association constant (K_a) of complexation for 1:1 stoichiometry (as determined through Job's plot) was estimated to be 1.13×10^{12} M^{-1}. Its comparison with that obtained for **L_2**-Pb^{2+} complex (log K_a =6.22 ± 0.24) in CH_3CN-H_2O (9.5:0.5 v/v) medium revealed that presence of aqueous component in medium lowers the extent of probe's coordination affinity for metal ions. Aqueous environment promotes for hydration of metal ions while probe-metal interaction is the driving force for complexation through an entropy-effect resulting from extra dehydration in inner-sphere complexes. Nevertheless, aqueous component has provided a suitable coordination environment to **L_2** for preferential complexation with Pb^{2+} ion while restricted other metal ions through their hydration to render selectivity in probe's signalling pattern.

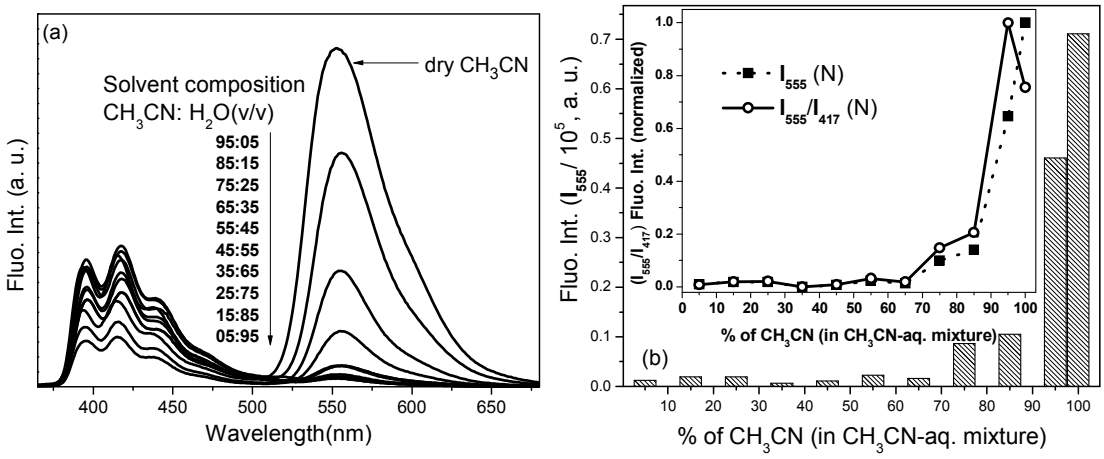

Fig. 6 (a) Fluorescence spectra and (b) corresponding intensity (I_{555}) of **L_2**-Pb^{2+} complex in various composition of CH_3CN-H_2O mixture, HEPES buffer, pH = 7.02, λ_{ex}= 350nm, em and ex bp = 5nm, RT, [**L_2**] =1μM, [Pb^{2+}] = 5μM; (Inset b): normalized fluorescence intensity ratio(I_{555}/I_{417}) showing optimal spectral enhancement in CH_3CN-H_2O::9.5:0.5 v/v composition.

In a controlled experiment, spectral changes of $\mathbf{L_2}$ were monitored in presence of Pb^{2+} in varying composition of aqueous (pH = 7.02, HEPES buffer) and CH_3CN components as solvent(Fig. 6) in order to determine appropriate aqueous-organic binary composition of solvent medium that facilitates the probe's optimal spectral perturbations and to explore the effect of aqueous component in promoting its selectivity. The preferential Pb^{2+} induced absorption(A_{525}) and fluorescence(I_{555}) enhancements pertaining to rhodamine's ring-opened conformation were observed to be optimal in dry CH_3CN. Among the binary mixtures, CH_3CN-H_2O (9.5:0.5 v/v) composition exhibited higher Pb^{2+} induced spectral amplifications, because, strong hydration ability of metal ion preferred its hydration in compositions with higher aqueous component over probe-metal interaction to induce none or negligible changes. However being a bifluorophoric probe, the ratiomeric signalling pattern of the FRET mediated I_{555} fluorescence enhancement upon excitation of $\mathbf{L_2}$-Pb^{2+} complex at 350nm revealed that fluorescence signal (I_{555}/I_{417}) ratio attained optimal in CH_3CN-H_2O (9.5: 0.5 v/v) composition(Inset, Fig. 6b), even higher than dry CH_3CN; which establishes the role of aqueous component and justifies appropriateness of composition in binary mixture in obtaining optimal spectroscopic changes.

The alteration in selectivity in metal ion induced dual mode signalling responses of these probes incorporating same receptor unit at carboxamide end, *i. e.* Hg^{2+} selectivity of $\mathbf{L_4}$ in comparison to that of Pb^{2+} in $\mathbf{L_1}$ under similar (aq.-organic) solvent condition attributed to stereo-electronic perturbation at receptor site originating from ethyl substitution at amino groups attached to xanthene core. Despite of having 2-aminoethyl pyridine substitution at carboxamide end in these probes, electron density drift to spirolactam carbonyl group from a tertiary amino group of rhodamine B (as in $\mathbf{L_4}$) presumed to be higher than that from a secondary one of rhodamine G (as in $\mathbf{L_1}$) and as a consequence, spatial disposition and coordination abilities of lactamide donors in receptor unit gets reoriented in $\mathbf{L_4}$ that modulate

binding preferences towards metal ions to exhibit an altered signalling responses when compared with that of $\mathbf{L_1}$. The partial substitution at one of –N(H)Et aniline segment of xanthene core in $\mathbf{L_1}$ functionalized with either bulky aromatics($\mathbf{L_2}$) or flexible long alkyl chains($\mathbf{L_2}$) might not have effected profound stereo-electronic modulation in comparison to $\mathbf{L_1}$ for such changes in binding preferences at receptor unit to exhibit subsequent altered metal ion selective spectral responses.

The reversibility in fluorescence signal responses of $\mathbf{L_2}$ due to metal ion induced FRET process was evaluated with subsequent addition of ammonium salts of various counter anions in CH_3CN-H_2O (9.5: 0.5 v/v) medium. The Pb^{2+} -induced enhancement in absorption (A_{527}) and emission (I_{550}) of $\mathbf{L_2}$ decreased almost to that of its metal free state and orange/green coloured solution turned colourless within 1 min. after addition of AcO^- anion. Addition of other counter anions exhibited a time dependent decrease in spectral responses and decolourization of its solution. Apart from anions, its spectral responses revealed that it regenerated its initial spirolactam state upon subsequent addition of chelating agents such as EDTA and ethylene diamine to $\mathbf{L_2}$-Pb^{2+} complex in solution. Subsequent addition of Pb^{2+} ions to the decolourized solution of anion(AcO^-) mediated Pb^{2+}-decomplexed $\mathbf{L_2}$ ($\Phi_{FT} \leq$ 0.002) resulted in its colourization again with re-appearance of enhanced A_{4527} and I_{550} spectral transitions almost to an extent of those upon initial Pb^{2+} addition to $\mathbf{L_2}$. This establishes its reusability as a probe for selective Pb^{2+} ion detection.

The ability of a probe to detect a metal ion selectively in presence of various competitive ones enables it to be a chemosensor for that particular metal ion. Hence, competitive experiments(Fig. 7a) were carried out for $\mathbf{L_2}$ in aq.-organic medium where addition of metal ions(5 equiv.) other than Pb^{2+} to the solution containing $\mathbf{L_2}$ and Pb^{2+} could not induce appreciable changes to its Pb^{2+} induced FRET mediated fluorescence emission (I_{550}) upon excitation at 350nm. However, solutions containing $\mathbf{L_2}$ and metal ions other than Pb^{2+}, which

exhibited none or negligible I_{550}, profoundly triggered FRET to enhance I_{550} when Pb^{2+} was added to it. Similar competitive experiments have established ability of **L_4** in selective detection of Hg^{2+} in aqueous-organic medium. The limit[26] of selective Pb^{2+} detection by **L_2** (LOD = 2.1 $\times 10^{-7}$ M) and Hg^{2+} detection by **L_4** (2.6 $\times 10^{-8}$ M) were estimated to be very low.

A faster response time for executing signalling action enables a probe to overcome associated implications for its practical implementation in real time monitoring. Hence, fluorescence spectral responses (I_{550}) of **L_2** upon excitation at 350nm were monitored as a function of time under in presence of varying concentrations of Pb^{2+}. Its Pb^{2+} induced FRET triggered I_{550} signals were observed to appear <1 min of addition of metal ions. Similarly, a faster response time (<1 min) of signalling was also obtained for **L_4** with Hg^{2+} ion. The spectroscopic signals corresponding to Pb^{2+} complexes of **L_1-L_3** and Hg^{2+} complex of **L_4** were found to be photo-stable as spectral pattern of solutions containing respective complexes remained enhanced at least up to 6h after irradiation at 350nm; retaining metal ion induced ring-opened conformation in these probes.

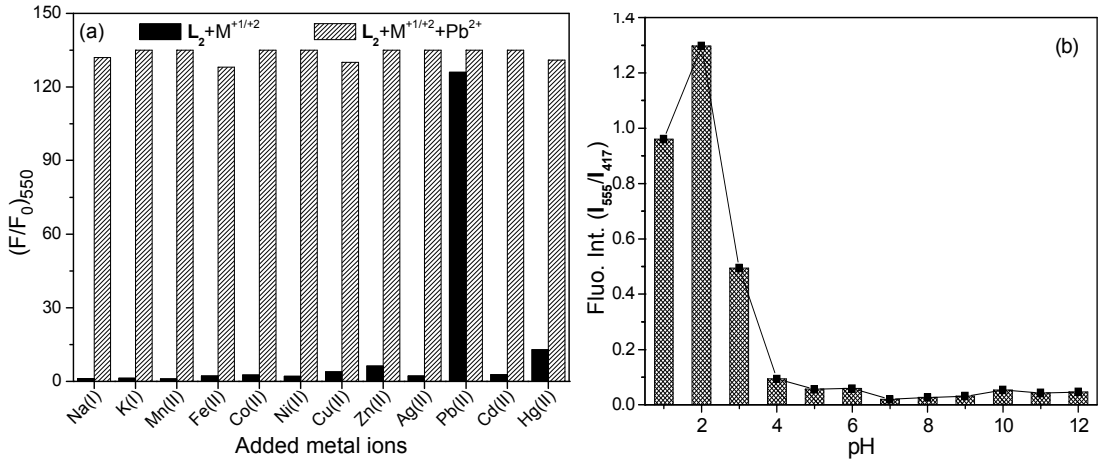

Fig. 7 (a) Fluorescence intensities of **L_2**- Pb^{2+} upon addition of various metal ions in CH_3CN-H_2O (9.5: 0.5 v/v) followed by subsequent addition of Pb^{2+} (5μM) ion, λ_{ex} = 350nm, [**L_2**]=1μM, [$M^{+1/+2}$] = 5μM. (b) Ratiomeric fluorescence signals of **L_2** in various pH showing its stability over a wide pH range.

The operational pH range of any probe for their metal ion induced optical spectral modulation is crucial in their practical implementation as chemosensors. Hence, absorption responses of these probes in absence and presence of Pb^{2+}/Hg^{2+} ion were monitored at varying pH. No I_{555} fluorescence in **L_2** was observed in 4-12 pH range(Fig. 7b) when excited at 350nm, suggesting its stability over a wider pH domain. However under highly acidic conditions(pH< 4), colour of **L_2** solution turned orange along with appearance of A_{528} absorption and I_{550} fluorescence transitions as a consequence of proton induced opening of its spiro-ring, apart from fluorescence enhancement at 393nm along with its vibrational structures originating from anthracene due to proton induced PET inhibition. In 5-10 pH range, addition Pb^{2+} led to its chromogenic and fluorogenic dual mode spectral amplifications through metal ion induced ring-opening and triggered FRET process, enabling these probes to be suitable for signalling operation under physiological conditions. Similarly, **L_4** was observed to exhibit signalling responses in presence of Hg^{2+} over a wider operational pH (4-12) range.

The effectiveness and utility assay of **L_2** in detection of Pb^{2+} ion was evaluated through monitoring its fluorescence signals in Pb^{2+} contaminated *E. Coli*(ESI). The microorganisms were incubated for 30 min at with **L_2** followed by addition of Pb^{2+} and vice-versa under physiological conditions. Their fluorescence imaging revealed that the non-fluorescent microorganism did not exhibit any rhodamine based emission when incubated with either only the probe or the metal ion. However, incubation with **L_2** followed by addition of Pb^{2+} led it to fluoresce upon excitation at 350nm. These observations hence demonstrated that **L_2** has potential for detection and quantification of Pb^{2+} ion accumulation in microorganisms and other biological functionalities.

Conclusion

In summary, photo-physical behaviour of $\mathbf{L_1}$ - $\mathbf{L_4}$ probes, which incorporate same receptor unit at their spirocyclic end but structurally vary as a function of substituents at one of amino-groups attached to their xanthene unit, were carried out to investigate effect of alkyl substitution on selectivity in their metal ion induced signalling pattern. The rhodamine G based probes ($\mathbf{L_1}$-$\mathbf{L_3}$) exhibited both chromogenic and fluorogenic signalling selectively in presence of Pb^{2+} ion in organic-aqueous medium through metal ion induced structural equilibration of their spiro-conformation. On contrary, rhodamine B based probe $\mathbf{L_4}$ exhibited similar dual mode signalling selectively in presence of Hg^{2+} ion under similar operational condition of solvent medium, which is in good agreement with that of other rhodamine based probes incorporating 'amino alkyl'- substitution at their spiro-cyclic end. The switching in selectivity between Pb^{2+} and Hg^{2+} ions in these probes as reflected in their signalling pattern is attributed to a perturbed stereo-electronic situation at receptor unit owing to partial substitution of various alkyl groups at amino N-atoms attached to xanthene core, which in turn, modulated the induced amine rigidity to perturb activation of internal conversion processes to various extent. Among rhodamine G based probes ($\mathbf{L_1}$-$\mathbf{L_3}$), extent of fluorescence enhancement selectively in presence of Pb^{2+} were observed in order of $\mathbf{L_1}$>$\mathbf{L_2}$≥$\mathbf{L_3}$, in concomitant correlation with the extent of induced rigidity at amino groups. Interesting among those is $\mathbf{L_2}$ which executed dual mode transduction selectively in presence of Pb^{2+} following FRET modulation pathways. The distinctive design of $\mathbf{L_2}$ incorporating the other fluorophore at aniline –N(H)Et segment of xanthene core differs from commonly designed FRET mediated rhodamine chemosensors[19a-d,20] where second fluorophore mostly attached at lactonized end. The ratiomeric fluorescent spectral module of $\mathbf{L_2}$ with Pb^{2+} enabled it to have a much lower detection limit, fulfilling pre-requisite criteria of subsequent chemosensing applications. Its extent of resonance energy transfer and its fluorescence decay

time were observed to be in alignment with its metal ion induced FRET modulated fluorescence enhancement. Signalling pattern in $\mathbf{L_2}$ responsive to multiple ions in acetonitrile in comparison with that to highly selective Pb^2 in aq.-acetonitrile medium inferred to the role of aqueous component in mixture medium in inducing selectivity, however, needs further investigation before ascertaining a concluding justification. Nevertheless, structural modifications at xanthene amino- groups in these probes effectively modulated the selectivity in metal ion coordination at receptor unit to subsequently alter chromogenic and fluorogenic signalling pattern for their detection at the desired low concentration level.

Acknowledgements

BPB wishes to thank DST, New Delhi for financial support (SB/EMEQ-226/2013) for this work; UGC New Delhi for a senior research fellowship to BB; the Director, CSIR-IMMT for infrastructural support through CSIR-CSC-0101.

Experimental Section

Synthesis:

9-(bromomethyl) anthracene: The compound was prepared from 9-hydroxymethylanthracene following a reported method[27].

$\mathbf{L_1}$: To a stirring solution of rhodamine 6G (0.445 g, 1 mmol) in ethanol (20 mL), 2-ethylamino pyridine (0.147 g, 1.2 mmol) was added and allowed to react for 24h at RT. The solvent was then evaporated under reduced pressure to obtain a brown semisolid residual mass. Water (50 mL) was added to residue and extracted with chloroform (3×50 mL). The combined organic layer were dried over anhydrous sodium sulphate, filtered and evaporated to dryness under reduced pressure to obtain a brown solid which was further purified by passing through a column of silica (100-200 mesh) with 1% methanol in chloroform(v/v) as eluent to yield $\mathbf{L_1}$ as the desired product.

Yield: 0.383g (73%); mixed m. p.= 94-96 °C; ESI-MS ($C_{33}H_{34}N_4O_2$): m/z$^+$(%), 519.25 [**L_1** +1]$^+$ (100), ^{1}H-NMR (400MHz, $CDCl_3$, 25° C, TMS, δ) : 8.54 (1H, d, *J* = 3.99 Hz), 8.35 (1H, d, *J* = 7.99 Hz), 7.93 (1H, d, *J* = 7.99 Hz), 7.59 (1H, dd, J_1 = 7.99 Hz, J_2 = 3.99 Hz), 7.43 (2H, t, *J* = 3.99 Hz), 7.13 (2H, dd, J_1 = 5.99 Hz, J_2 = 3.99 Hz), 6.98 (1H, d, *J* = 7.99 Hz), 6.35 (2H, s), 6.23 (1H, s), 3.48 (2H, dt, J_1 = 7.99 Hz, J_2 = 1.99 Hz), 3.19 (2H, dd, J_1 = 5.99 Hz, J_2 = 3.99 Hz), 3.11 (2H, t, *J* = 3.99 Hz), 2.92 (2H, t, *J* = 7.99 Hz), 2.68 (2H, d, *J* = 5.99 Hz), 1.84 (4H, d, *J* = 7.99 Hz), 1.30 (6H, t, *J* = 6.99 Hz); ^{13}C-NMR(400MHz, $CDCl_3$, 25° C, TMS, δ): 160.04, 151.70, 149.35, 148.91, 147.33, 136.37, 136.04, 132.36, 131.06, 128.50, 127.91, 123.71, 123.39, 123.15, 122.72, 121.28, 120.99, 117.81, 106.04, 96.63, 65.10, 41.92, 40.23, 38.34, 36.57, 16.69, 14.79. Anal calcd for $C_{33}H_{34}N_4O_2$(M_w = 518.65), %: C, 76.42, H, 6.61, N, 10.80; found: C, 75.97, H, 6.79, N, 10.93.

L_2: To a stirring solution of **L_1** (0.519 g, 1 mmol) in toluene (50 mL), Et_3N (0.28 mL, 2mmol, excess) was added followed by 9-bromomethyl anthracene (0.272 g, 1 mmol) and heated to reflux for 8 h. The solution mixture was then cooled to room temperature, filtered and the solvent was evaporated under reduced pressure. Water (30 mL) was added to the brown solid and extracted with $CHCl_3$ (3×30 mL). The combined organic layer, after drying over anhydrous Na_2SO_4, were evaporated to dryness under reduced pressure to obtain the desired product as brown solid which was further purified by passing through a column (100–200 mesh silica gel) with chloroform and methanol (99 : 1 v/v) as eluent.

Yield: 0.604g (84%); mixed m. p.= 123-126 °C; ESI-MS ($C_{48}H_{44}N_4O_2$): m/z$^+$(%), 709.24 [**L_2** +1]$^+$ (25%); ^{1}H-NMR (400MHz, $CDCl_3$, 25° C, TMS, δ): 8.60 (1H, d, *J* = 3.99 Hz), 8.43 (1H, s), 8.36 (1H, d, *J* = 7.99 Hz), 8.20 (1H, d, *J* = 7.99 Hz), 7.93 (1H, d, *J* = 7.99 Hz), 7.54 (2H, s), 7.40 (4H, q, *J* = 3.99 Hz), 7.36 (2H, d, *J* = 7.99 Hz), 7.28 (2H, br s), 6.98 (1H, d, *J* = 7.99 Hz), 6.40 (2H, s), 6.35 (1H, br s), 6.23 (1H, br s), 5.66 (1H, s), 4.65 (1H, s), 3.50 (2H, t, *J* = 3.99 Hz), 3.19 (2H, d, *J* = 3.99 Hz), 2.72 (2H, t, *J* = 3.99 Hz), 1.86 (4H, d, *J* = 7.99 Hz), 1.78

(2H, s), 1.32 (2H, d, J = 3.99 Hz), 1.29 (2H, d, J = 7.99 Hz), 0.88 (6H, br s); ^{13}C-NMR(400MHz, $CDCl_3$, 25° C, TMS, δ): 168.39, 151.71, 149.81, 148.93, 147.34, 136.04, 132.38, 131.47, 131.31, 129.08, 128.87, 128.81, 128.51, 127.93, 127.52, 126.36, 125.54, 125.34, 125.30, 125.05, 124.82, 124.76, 124.72, 124.01, 123.78, 123.16, 122.73, 120.99, 65.11, 40.22, 38.35, 36.59, 16.72, 14.74; Anal calcd for $C_{48}H_{44}N_4O_2$(M_w = 708.89), %: C, 81.33, H, 6.26, N, 7.90; found: C, 81.19, H, 6.10, N, 8.07.

L_3: To a stirring solution of **L_1** (0.520 g, 1 mmol) in toluene (50 mL), Et_3N (0.28 mL, 2mmol, excess) was added followed by 1-bromo octane (0.190 g, 1 mmol) and heated to reflux for 16 h. The solution mixture was then cooled to room temperature, filtered and solvent was removed under reduced pressure. Water (30 mL) was added to the brown solid and extracted with $CHCl_3$ (3×30 mL). The combined organic layer, after drying over anhydrous Na_2SO_4, were evaporated to dryness under reduced pressure to obtain the desired product as brown solid which was further purified by passing through a column (100–200 mesh silica gel) with chloroform and methanol (99 : 1 v/v) as eluent.

Yield: 0.538g (85%); mixed m. p.= 113-116 °C; ESI-MS ($C_{41}H_{50}N_4O_2$): m/z$^+$ (%), 631.27 [**L_3**+1]$^+$(63%); ^{1}H-NMR (400MHz, $CDCl_3$, 25° C, TMS, δ): 8.35 (1H, s), 8.28 (1H, s), 7.85 (1H, dd, J_1 = 3.79 Hz, J_2 = 1.59 Hz), 7.55 (1H, dt, J_1 = 3.79 Hz, J_2 = 1.59 Hz), 7.35 (1H, td, J_1 = 3.99 Hz, J_2 = 1.59 Hz), 7.17 (1H, d, J = 5.59 Hz), 7.10 (1H, d, J = 3.19 Hz), 6.95 (1H, dd, J_1 = 3.99 Hz, J_2 = 1.19 Hz), 6.92 (1H, d, J = 1.19 Hz), 6.86 (1H, d, J = 7.59 Hz), 6.29 (1H, s), 6.14 (1H, s), 5.72 (1H, br s), 3.50 (2H, t, J = 4.79 Hz), 3.40 (2H, s), 3.32 (4H, dt, J_1 = 7.99 Hz, J_2 = 1.59 Hz), 3.09 (4H, br s), 2.94 (4H, t, J = 7.19 Hz), 2.68 (2H, d, J = 5.59 Hz), 2.57 (2H, t, J = 7.59 Hz), 1.80 (6H, s), 1.29 (2H, d, J = 5.59 Hz), 1.21 (6H, td, J_1 = 7.19 Hz, J_2 = 1.59 Hz), 0.80 (3H, br s); ^{13}C-NMR (400MHz, $CDCl_3$, 25° C, TMS, δ): 168.17, 159.06, 158.87, 157.96, 153.74, 151.68, 149.07, 148.93, 137.34, 136.66, 132.43, 130.96, 128.36, 127.97, 123.80, 122.65, 121.59, 117.85, 105.75, 96.50, 65.18, 53.48, 47.94, 46.98, 40.30,

38.27, 36.49, 34.82, 33.86, 32.75, 31.69, 29.24, 28.93, 27.16, 26.68, 25.34, 22.54, 16.72, 14.66, 14.03; Anal calcd for $C_{41}H_{50}N_4O_2$(M_w = 630.35), %: C, 78.06, H, 7.99, N, 8.88, found: C, 77.91, H, 8.11, N, 8.99.

L_4: To a stirring solution of rhodamine B hydrochloride (0.478 g, 1 mmol) in EtOH(50 mL), an ethanolic (20mL) solution of 2-aminoethyl pyridine (0.610 g, 5 mmol, excess) was added and heated to reflux for 10 h., after which the reaction mixture was cooled at room temperature and solvent was evaporated under reduced pressure. Water (50 mL) was added to the brown solid and extracted with $CHCl_3$ (3×30 mL). The combined organic layers, after drying over anhydrous Na_2SO_4, were evaporated to dryness under reduced pressure to obtain the desired product **L_4** as brown solid. It was further dissolved in warm ethanol, which on slow evaporation afforded blocked shaped colourless single crystals suitable for X-ray diffraction.

Yield: 0.710g (69%); mixed m. p.= 103-106 °C; ESI-MS ($C_{35}H_{38}N_4O_2$) m/z$^+$ (%): 583.15 [**L_4** .HCl]$^+$ (100); ^{1}H-NMR (400MHz, $CDCl_3$, 25° C, TMS, δ): 8.53 (1H, d, *J* = 3.99 Hz), 8.48 (1H, d, *J* = 5.99 Hz), 7.92 (1H, d, *J* = 7.99 Hz), 7.61 (1H, d, *J* = 1.99 Hz), 7.41 (1H, d, *J* = 7.99 Hz), 7.12 (2H, td, J_1 = 7.99 Hz, J_2 = 3.59 Hz), 6.99 (1H, s), 6.43 (2H, d, *J* = 7.99 Hz), 6.38 (2H, d, *J* = 3.99 Hz), 6.23 (2H, d, *J* = 7.99 Hz), 3.30 (2H, t, *J* = 7.99 Hz), 3.12 (2H, t, *J* = 7.99 Hz), 2.95 (4H, d, *J* = 7.99 Hz), 2.92 (4H, d, *J* = 7.99 Hz), 1.18 (12H, t, *J* = 7.99 Hz); ^{13}C-NMR(400MHz, $CDCl_3$, 25 °C, TMS, δ): 168.21, 159.6(d), 153.81(d), 149.38(d), 148.92(m), 137.26, 136.73(m), 132.33, 131.09, 128.82, 127.94, 126.05, 123.72(m), 122.70(d), 121.68(m), 108.03, 105.48, 97.77, 65.05, 44.32, 40.65(d), 39.91(d), 36.60, 12.60; Anal. calcd. for $C_{35}H_{38}N_4O_2$(M_w = 546.70), %: C, 76.89, H, 7.01, N, 10.25, found: C, 76.43, H, 7.16, N, 10.15.

Notes and references

‡ Crystallographic data for **L_4**: $C_{35}H_{38}N_4O_2$; M_w = 546.69; block-shaped; colourless, orthorhombic, space group P n a 2_1, a = 13.399(2) Å, b = 15.319(7)Å, c = 13.902(9) Å, $\alpha = \beta = \gamma = 90.00$, U = 2853.1(6)Å^3, T = 100(2) K, Z = 4, μ(Mo K_α) = 0.080 mm^{-1}, F(000) = 1168, ρ_{calc} = 1.273mg/m^3, 7051 reflection data with 370 parameters, 3823 [I ≥ 2 σ(I)] unique reflections used in calculations. The final R_1 = 0.0882, wR_2 = 0.1827, S = 0.997. (CCDC No. 963835).

1. For reviews, see: (a) J. S. Kim and D. T. Quang, *Chem. Rev.*, 2007, **107**, 3780; (b) B. Bag and P. K. Bharadwaj, in *Photo, Electrochemistry & Photobiology in the Environment, Energy and Fuel*, S. Kaneco (ed.), 2007, 201; (c) V. Amendola, L. Fabbrizzi, F. Forti, M. Licchelli, C. Mangano, P. Pallavicini, A. Poggi, D. Sacchi and A. Taglieti, *Coord. Chem. Rev.*, 2006, **250**, 273; (d) J. F. Callan, A. P. de Silva and D. C. Magri, *Tetrahedron*, 2005, **61**, 8551; (e) B. Valeur and I. Leroy, *Coord. Chem. Rev*., 2000, **205**, 3; (f) A. P. de Silva, H. Q. N. Gunaratne, T. Gunnlauggsson, A. J. M. Huxley, C. P. McCoy, J. T. Radmacher and T. E. Rice, *Chem. Rev.*, 1997, **97**, 1515.
2. (a) *Heavy Metals in the Environment*, B. Sarkar (ed.), Marcel Dekker Inc., New York, 2002; (b) D. Beyersmann, in *Metals and Their Compounds in the Environment*, E. Merian (ed.), Wiley-VCH: Weinheim, 1990; (c) W. F. Fitzgerald, C. H. Lamborg and C. R. Hammerschmidt, *Chem. Rev*., 2007, **107**, 641; (d) T. W. Clarkson and L. Magos, *Crit. Rev. Toxicol.*, 2006, **36**, 609; (e) O. Malm, *Environ. Res*., 1998, **77**, 73; (f) P. Grandjean, P. Weihe, R. F. White and F. Debes, *Environ. Res.*, 1998, **77**, 165.
3. (a)H. L. Needleman, *Human Lead Exposure*, CRC Press, Boca Raton, FL, 1992; (b)J. D. Cremin, Jr., M. L. Luck, N. K. Laughlin and D. R. Smith, *Toxicol. Appl. Pharmacol.*, 1999, **161**, 283; (c)Y. Finkelstein, M. E. Markowitz and J. F. Rosen, *Brain Res. Rev.*, 1998, **27**, 168.
4. (a) T. I. Lidsky and J. S. Schneider, *Brain*, 2003, **126**, 5; (b) H. -W. Tang, G. Huel, D. Campagna, G. Hellier, C. Boissinot and P. Blot, *J. Appl. Toxicol*., 1999, **19**,167; (c) L. Stokes, R. Letz, F. Gerr, M. Kolczak, F. E. McNeill, D. R. Chettle and W. E. Kaye, *Occup. Environ. Med*., 1998, **55**, 507; (d) K. M. Stiles and D. C. Bellinger, *Neurotoxicol. Teratol*., 1993, **15**, 27.
5. E. K. Silbergeld, I. A. Silva and J. F. Nyland, *Toxicol. Appl. Pharmacol.,* 2005, **207**, S282.

6. P. Kaur, M. Aschner and T. Syversen, *Neurotoxicol.*, 2006, **27**, 492; (b) E. R. Milaeva,. *J. Inorg. Biochem.*, 2006, **100**, 905; (c) R. K. Zalups and S. Ahmad, *J. Am. Soc. Nephrol.*, 2004, **15**, 2023; (e) R. K. Zalups and L. H. Lash, *Toxicol. Appl. Pharmacol.*, 2006, **214**, 88; (d) G. Shanker, L. A. Mutkus, S. J. Walker and M. Aschner, *Mol. Brain Res.*, 2002, **106**, 1.
7. I. Oniyido, A. R. Norris and E. Buncel, *Chem. Rev.*, 2004, **104**, 5911; (b) H. H. Harris, I. J. Pickering and G. N. George, *Science*, 2003, **301**, 1203; (c) D. W. Boening, *Chemosphere*, 2000, **40**, 1335.
8. For selected reviews, see: (a) L.Yuan, W. Lin, K. Zheng, L. He and W. Hyang, *Chem. Soc. Rev.*, 2013, **42**, 622; (b) X. Chen, T. Pradhan, F. Wang, J. S. Kim and J. Yoon, *Chem. Rev*., 2012, **112**, 1910; (c) M. Beija, C. A. M. Afonso and J. M. G. Martinho, *Chem. Soc. Rev*., 2009, **38**, 2410; (d) J. F. Jhang and J. S. Kim, *Anal. Sci*., 2009, **25**, 1271; (e) H. N. Kim, M. H. Lee, H. J. Kim, J. S. Kim and J. Yoon, *Chem. Soc. Rev.*, 2008, **37**, 1465.
9. Few recent examples for Hg^{2+} ions: (a) X. Chen, X. Meng, S. Wang, Y. Cai, Y. Wu, Y. Feng, M. Zhu and Q. Guo, *Dalton trans*., 2013, **42**, 14819; (b) W. Wang, Y. Li, M. Sun, C. Zhou, Y. Zhang, Y. Li and Q. Yang, *Chem. Commun.,* 2012, **48**, 6040; (b) K. Ghosh, T. Sarkar, A. Sammader, *Org. Biomol. Chem*., 2012, **10**, 3236; (c) F. Wang, S.-W. Nam, Z. Guo, S. Park and J. Yoon, *Sens. Actuat. B*, 2012, **161**, 948; (d) S. Saha, P. Mahato, G. U. Reddy, E. Suresh, A. Chakrabarty, M. Baidya, S. K. Ghosh and A. Das, *Inorg. Chem*., 2012, **51**, 336; (e) N. Vasimalai and S. A. John, *Analyst*, 2012, **137**, 3349.
10. Pb^{2+} ions: (a) Z.-Q. Hu, C.-S Lin, X.-M. Wang, L. Ding, C.-L. Cui, S.-F. Liu and H. Y. Lu, *Chem. Commun*., 2010, **46**, 3765; (b) X. Zhang, Y. Shiraishi. T. Hirai, *Tetrahedron Lett*., 2007, **48**, 5455; (c) J. Y. Kwon, Y. J. Jang, Y. J. Lee, K. M. Kim, M. S. Seo, W. Nam. J. Yoon, *J. Am. Chem. Soc*., 2005, **127**, 10107.
11. (a) B. Bag and B. Biswal, *Org. Biomol. Chem.*, 2012, **10**, 2733; (b) A. Pal and B. Bag, *J. Photochem. Photobiol A*, 2012, **240**, 42; (c) B. Bag and A. Pal, *Org. Biomol. Chem.*, 2011, **9**, 4467.
12. (a) X. Zhang, Y. Xiao and X. Qian, *Angew. Chem., Int. Ed*., 2008, **47,** 8025; (b) J. V. Mello and N. S. Finney, *Angew. Chem., Int. Ed. 2001*, **40**, 1536; (c) H. Takakusa, K. Kikuchi, Y. Urano, H. Kojima and T. Nagano, *Chem. Eur. J.*, 2003, **9**, 1479; (d) A. Coskun and E.U. Akkaya, J. *Am. Chem. Soc*., 2005, **127**, 10464; (e) W. Lin, L. Yuan, L. Long, C. Guo and J. Feng, *Adv. Funct. Mater*., 2008, **18**, 2366; (f) Z. Xu, X. Qian and J. Cui, *Org. Lett*., 2005, **7**, 3029.

13. (a) F. D. Lewis, Y. Zhang, and R. L. Letsinger, *J. Am. Chem. Soc.* 1997, **119**, 5451; (b) J. Lou, T. A. Hatton, and P. E. Laibinis, *Anal. Chem*. 1997, **69**, 1262; (c) A. T. Reise Sousa, E. M. S. Castanheira, A. Fedorov, and J. M. G. Martinho, *J. Phys. Chem. A,* 1998, **102**, 6406; (d) H. Nohta, H. Satozono, K. Koiso, H. Yoshida, ,J. Ishida, and M. Yamaguchi, *Anal. Chem*. 2000, **72**, 4199; (e) A. Okamoto, T. Ichiba, and I. Saito, *J. Am. Chem. Soc*. 2004, **126**, 8364.

14. (a) C. Kaewtong, B. Wanno, Y. Uppa, N. Morakot, B. Pulpoka and T. Tuntulani, *Dalton trans*., 2011, **40**, 12578, (b) Y. H. Lee, M. H. Lee, J. F. Zhang and J. S. Kim, *J. Org. Chem*., 2010, **75**, 7159; (c) S. K. Kim, K. M. K. Swamy, S.-Y. Chung, H. N. Kim, M. J. Kim, Y, Jeong and J. Yoon, *Tetrahedron Lett*., 2010, **51**, 3286; (d) J. Mao, L. Wang, W. Dou, X. Tang, Y. Yan and W. Liu, *Org. Lett*., 2007, **9**, 4567.

15. (a) T. Lopez Arbeloa, F. Lopez Arbeloa, M. J. Estevez and F. Lopez Arbeloa, *J. Lumin*., 1994, **59**, 369; (b) M. Vogel, W. Rettig, R. Sens and K.H. Drexhage, *Chem. Phys. Lett*., 1988, **147**, 452; (c) M. Vogel, W. Rettig, R. Sens and K.H. Drexhage, *Chem. Phys. Lett*., 1988, **147**, 461; (d) T. Karstens and K. Kobs, *J. Phys. Chem.*, 1980, **84**, 1871.

16. (a) B. Bag, P. K. Bharadwaj, *J. Phys. Chem. B*, 2005, **109**, 4377; (b) J. S. Kim, K. H. Noh, S. H. Lee, S. K. Kim, and J. Yoon, *J. Org. Chem.*, *2003*, **68**, 597; (c) L. Aoki,; T. Sakaki, and S. Shinkai, *J. Chem. Soc., Chem. Commun*., 1992, 730.

17. (a) *Advanced Concepts in Fluorescence Spectroscopy*: *Small Molecule Sensing*, C.D. Geddes and J. R. Lakowicz (eds.), Springer-Sciences, New York, USA, 2005; (b) G. J. Kavarnos, *Fundamentals of Photoinduced Electron Transfer*, VCH, Weinheim, 1993; (c) K. Bhattacharyya and M. Chowdhury, *Chem. Rev*., 1993, **93**, 507; (d) F. Fages, J. –P. Desvergne and H. Bouas–Laurent, *J. Am. Chem. Soc*., 1989, **111**, 96; (e) C. D. Rehm and A. Weller, *Isr. J. Chem*., 1970, **8**, 259.

18. (a) K. Kikuchi, *Chem. Soc. Rev*., 2010, **39**, 2048, (b) K. E. Sapsford, L. Berti and I. L. Medintz, *Angew. Chem. Int. Ed*., 2006, **45**, 4562; (c) J. N. Miller, *analyst*, 2005, **130**, 265; (d) K. E. Sapsford, L. Berti and I. L. Medintz, *Angew. Chem. Int. Ed.*, 2006, **45**, 4562; (e) *Topics in Fluorescence Spectroscopy*, J. R. Lakowicz (ed.), Plenum press, New York, 1999; (f) T. Förster, *Z. Naturforsch*. *A*, 1949, **49**, 321.

19. (a) N. R. Chereddy, S.Thennarasu and A. B. Mandal, *Analyst*, 2013, **138**, 1334; (b) B. Liu, F. Zeng, Y. Liua and S. Wu, *Analyst*, 2012, **137**, 1698 (c) V. Luxami, M. Verma, R. Rani, K. Paul and S. Kumar, Org. Biomol. Chem., 2012, **10**, 8076; (d) X. Lv, J. Liu, Y. Liu, Y. Zhao, M. Chen, P. Wang and W. Guo, *Org. Biomol. Chem.*, 2011, **9**, 4954; (e) R.

Ferreira, P. Remo´n and U. Pischel, *J. Phys. Chem. C*, 2009**, 113***,* 5805; (f) E. S. Barrett, T. J. Dale and J. Rebek Jr.*, J. Am. Chem. Soc*., 2007, **129**, 3818; (g) K. K. Sadhu, B. Bag and P. K. Bharadwaj, *Inorg. Chem.*, 2007, **46**, 8051; (h) A. E. Albers, V. S. Okreglak and C. J. Chang, J. *Am. Chem. Soc*. 2006, **128**, 9640; (i) A. Ono and H. Togashi, *Angew. Chem., Int. Ed.*, 2004, **43**, 4300.

20. B. Biswal and B. Bag, *Org. Biomol. Chem*., 2013, **11**, 4975.
21. R. Menzel, R. Bornemann and E. Thiel, *Phys. Chem. Chem. Phys*., 1999, **1**, 2435; (b) R. Menzel and E. Thiel, *Chem. Phys. Lett*., 1998, **291**, 237, (c) J. Karpiuk, Z. R. Grabowski and F. C. De Schryver, *J. Phys. Chem*., 1994, **98**, 3247.
22. (a) P. Thordarson, *Chem. Soc. Rev*., 2011, **40**, 1305; (b) Y. Shiraishi, S. Sumiya, Y. Kohno and T. Hirai, *J. Org. Chem.,* 2008, **73**, 8571; (c) S. Fery-Forgues, M. -T. Le-Bris, J.-P. Guette and B. Valeur, *J. Phys. Chem.*, 1988, **92**, 6233, (d) H. A. Benesi and J. H. Hildebrand, *J. Am. Chem. Soc*., 1949, **71**, 2703.
23. (a) B. Valeur, *Molecular Fluorescence: Principles and Applications*, Wiley–VCH, 2002, p 247; (b) K. Kils, J. Kajanus, J. Mrtensson and B. Albinsson, *J. Phys. Chem. B*, 1999, **103**, 7329; (c) K. K. Jensen, S. B. van Berlekom, J. Kajanus, J. Mrtensson and B. Albinsson, *J. Phys. Chem. A*, 1997, **101**, 2218.
24. (a) P. Mahato, S. Saha, E. Suresh, R. Di Liddo, P. P. Parnigotto, M. T. Conconi, M. K. Kesharwani, B. Ganguly and A. Das, *Inorg. Chem*., 2012, **51**, 1769; (b) C. Ma, F. Zeng, L. Huang and S. Wu, *J. Phys. Chem. B*, 2011, **115**, 874; (c) B. Ma, S. Wu, Y. Luo, J. Zhao and Z. Tong, *Nanotechnology*, 2010, **21**, 195501.
25. C. G. dos Remedios and P. D. Moens, *J. Struct. Biol*., 1995, **115**, 175.
26. (a) C. R. Lohani, J.-M. Kim, S-Y. Chung, J. Yoon, and K.- H. Lee, *Analyst*, 2010, **135**, 2079, (b) B. P. Joshi, C. R. Lohani and K.- H. Lee, *Org. Biomol. Chem.*, 2010, **8**, 3220.
27. M. Bullpit, W. Kitching, D. Doddrell and W. J. Adcock, *Org. Chem*., 1976, **41**, 760.

Switching selectivity between Pb^{2+} and Hg^{+2} ions through variation of substituents at xanthene end; 'turn-on' signalling responses by FRET modulation

Biswonath Biswal and Bamaprasad Bag*

Colloids and Materials Chemistry Department, Academy of Scientific and Innovative Research, CSIR-Institute of Minerals and Materials Technology, P.O.: R.R.L., Bhubaneswar-751 013, Odisha, India. Fax: (+) 91 674 258 1637; Tel: (+ 91) 674 237 9254, Email: *bpbag@immt.res.in*

Graphical Abstract for table of contents

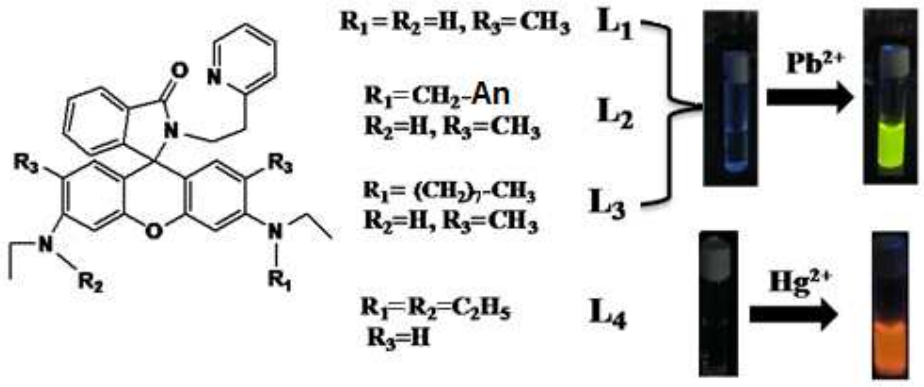

In a dual mode rhodamine based signalling probe, selectivity switches from Pb^{2+} to Hg^{2+} as a function of substitution at amino groups attached to xanthene core through stereo-electronic modulation of aminoethyl receptor at spirocyclic end; FRET mediated signalling with distinctive integration of other fluorophore at substituted aniline segment of its xanthene core.